NASA/TM-1998-207683

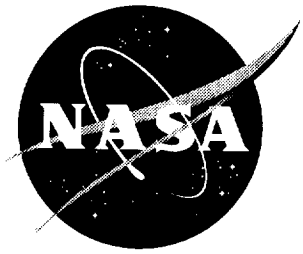

Experimental and Theoretical Study of Flow Fields Around Ducted-Nacelle Models

Robert J. Mack
Langley Research Center, Hampton, Virginia

National Aeronautics and
Space Administration

Langley Research Center
Hampton, Virginia 23681-2199

May 1998

Available from the following:

NASA Center for AeroSpace Information (CASI)
7121 Standard Drive
Hanover, MD 21076-1320
(301) 621-0390

National Technical Information Service (NTIS)
5285 Port Royal Road
Springfield, VA 22161-2171
(703) 487-4650

Experimental And Theoretical Study Of Flow Fields Around Ducted-Nacelle Models

Robert J. Mack

Langley Research Center

Hampton, Virginia

SUMMARY

The flow field near four small-scale ducted-nacelle bodies of revolution has been analytically and experimentally studied to determine exterior and interior mass-flow characteristics, and to measure flow-field overpressures generated by the nacelle's forebody shape. Four nacelle models with the same profile, but of different sizes, were used in the study. Shadowgraph pictures showed inlet shocks attached to the cowl lip (indicating unchoked flow) on all four models, at all the test Mach numbers, through an angle of attack range of 0.0 to 6.0 degrees. Pressure signatures measured in the flow field of the largest of the four nacelle models were compared with those predicted by corrected and uncorrected Whitham theory. At separation distances greater than 3.0 to 4.0 inlet diameters, good agreement was found. Poorer agreement was found at extreme near-field separation distances, but this was attributed to pressure-gage limitations and probe-flow field interactions. The overall favorable results supported a conclusion that corrected Whitham theory was sufficiently accurate to make the nacelle-wing interference-lift code useful for sonic-boom analysis and the preliminary design of supersonic-cruise conceptual aircraft.

INTRODUCTION

Some of the analytic tools, references 1 to 5, useful in analyzing and optimizing wings and wing-fuselage configurations, were developed approximately 30 years ago. They were some of the "cutting-edge-of-technology" codes used in the National Supersonic Transport Program during the middle 1960's. New methods were also developed to optimize the integration of engine nacelles with a configuration's wing and fuselage. With the earlier methods, engine nacelles were usually aerodynamically integrated, using techniques which emphasized minimum configuration drag. After 1969, computer-code methods, references 6 and 7, became available that could computationally predict nacelle-wing interference lift, drag, and pitching moment increments on conceptual aircraft with wing-mounted nacelles. In addition to calculating aerodynamic forces and pitching moment, the Langley code, reference 6, could calculate area-ruled nacelle-wing interference lift distributions for use in sonic-boom analysis.

These nacelle-wing interference lift codes were based on the application of Whitham theory, reference 8, to ducted bodies of revolution. Validation of theory with experiment was done using existing wind-tunnel test data of flow-field overpressures measured from pointed slender bodies of revolution. Most of these early wind-tunnel tests were far-field overpressure measurements. When the wind-tunnel models were slender, good agreement between theory and experiment was found. So, the region of study shifted from the far-field toward the near-field to determine the full capabilities and limitations of Whitham theory. New methods, reference 9, were developed to readily obtain pressure signature predictions by numerical calculation. References 10 through 13 presented results with a range of agreement between theory and experiment in a small sample of early sonic-boom research. This data base included measurements of flow-field pressures around a slender ducted-nacelle, reference 6, which proved to be useful in later studies.

The capability to quickly predict nacelle-wing interference forces and moments proved useful in the design and analysis of wing-fuselage-nacelle configurations of conceptual supersonic-cruise aircraft. Predictions of nacelle-wing interference lift were also employed for the design and the sonic-boom analysis of low-boom, shaped-pressure-signature aircraft concepts. Validating these desirable capabilities prompted the design, construction, and testing of a multi-duct wind-tunnel model to measure near-field pressures around nacelles, and to determine conditions which fostered unchoked flow through the internal ducts of the small nacelles used on wind-tunnel models.

In this paper, the design of this multi-ducted-nacelle wind-tunnel model is described. The pressure signature measurement apparatus, its arrangement in the test section, wind-tunnel test conditions, and test procedures are also documented. Measurements of flow-field overpressures made over a range of separation distances and Mach numbers are presented and analyzed. Samples of the measured pressure signatures are compared with predicted pressure signatures obtained from Whitham theory and a corrected Whitham theory which is the basis for the nacelle-wing interference-lift codes. The results from these comparisons are analyzed and discussed to judge the capabilities and the applicability of the Langley nacelle-wing interference-lift code.

SYMBOLS

D_{max} maximum nacelle model diameter, inches

D_{min} minimum nacelle model diameter, i.e. inlet diameter, inches

F(y) Whitham F-function of parameter y

$\Delta F(y)$ incremental "jump" in a F(y) function due to an expansion or a shock

h separation distance between nacelle model center line and survey probe in a plane normal to the test-section wall, inches

l overall length of ducted nacelle, inches

l_f nacelle-model forebody length, inches

M Mach number

Δp flow-field overpressure, psf

p ambient pressure, psf

R nacelle radius, inches

x longitudinal distance, inches

y effective length in the longitudinal direction, inches

β Mach number parameter, $\sqrt{M^2 - 1.0}$

γ ratio of specific heats for air, assumed to be 1.4

δ flow deflection angle through an oblique shock or the nacelle inlet-lip angle, deg

κ coefficient defined in equation (A4); used in equations (3) and (A6)

ξ linear-theory ratio of incremental pressure rise to ambient pressure

MODELS

The four ducted-nacelle models used in the wind-tunnel overpressure measurement tests had the nacelle shape shown schematically in figure 1.

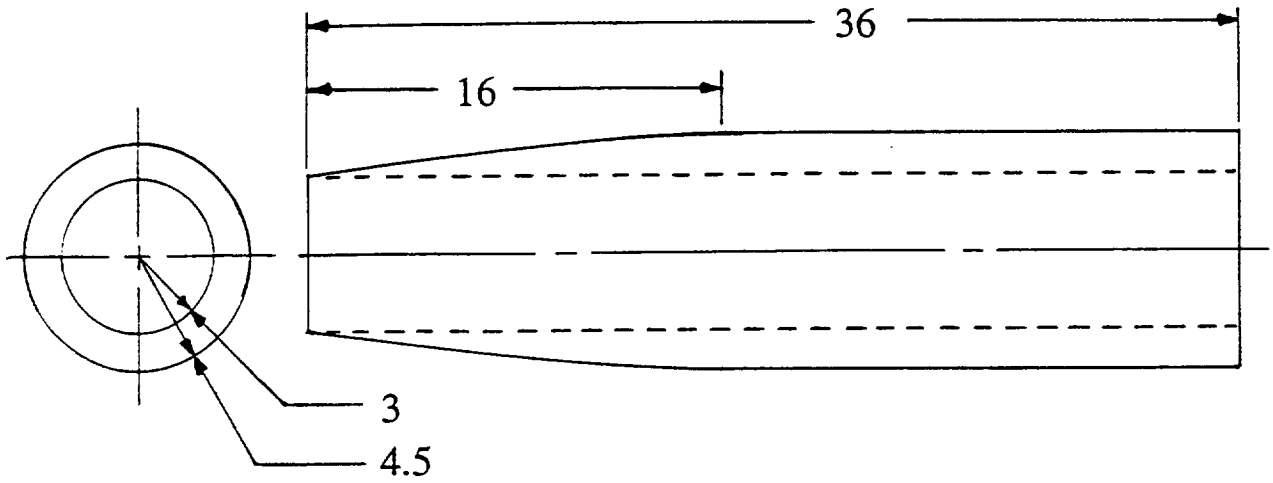

Figure 1. Ducted-nacelle shape used on the four wind-tunnel models. *Dimensions in feet.*

The length of the nacelle was approximately that of a nacelle on a full-scale conceptual aircraft. On each model, the ratio of (overall length)/(inlet diameter) was 6:1, the ratio of (minimum diameter)/(maximum diameter) was 2:3, and the ratio of (forebody length)/(overall length) was 4:9. The nacelle-inlet-lip angle was $tan^{-1}(0.1875) = 10.62$ *degrees*; large enough to generate noticeable inlet-lip shocks on the shadowgraph pictures and be relatively easy to build. This lip angle was generous in size since those usually found on the inlets of high speed civil transport (HSCT) concepts were usually about 3.0 to 4.0 degrees. A constant-area duct, with a diameter equal to the inlet diameter, went through the center of each nacelle. The equations that defined the full-scale nacelle shape were:

$$R = 3.0 + \frac{3}{16}x - \frac{3}{512}x^2 \text{ ft} \quad : \quad 0 \le x \le 16 \text{ ft}$$

$$R = 4.5 \text{ ft} \quad : \quad 16 \le x \le 36 \text{ ft}.$$

Scale factors of 1:75, 1:100, 1:150, and 1:200 were used to build the set of ducted-nacelle models with characteristic dimensions described in Table I.

Table I. Characteristic dimensions, in inches, of the four ducted-nacelle models

Scale Factor	D_{min}, in	D_{max}, in	l_f, in	l, in
1 : 75	0.96	1.44	2.56	5.76
1 : 100	0.72	1.08	1.92	4.32
1 : 150	0.48	0.72	1.28	2.88
1 : 200	0.36	0.54	0.96	2.16

The four models were strut-mounted, cruciform fashion, on an ogive-nosed center body, figure 2, for ease of positioning during the tests. Models, struts, and center body were made of stainless steel.

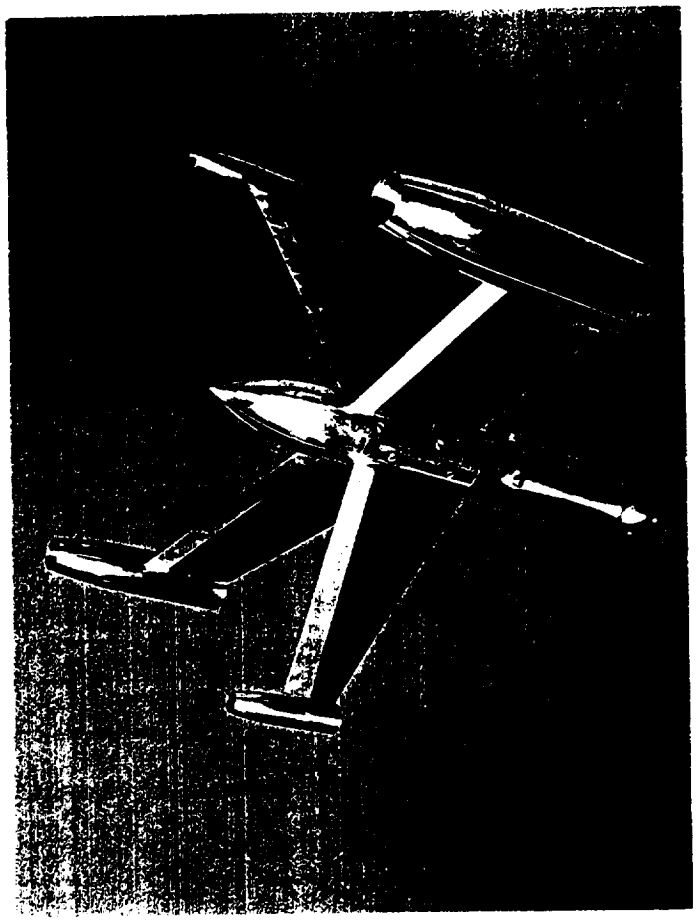

Figure 2. Cruciform-strut mounted ducted-nacelle model.

Shadowgraph pictures were made of all four nacelles in supersonic flow. However, only the largest of the four nacelle models was used to obtain measurements of flow-field overpressure disturbances. The location of the nacelle strut which held the model precluded the measurement of overpressure signatures over the entire length of the nacelle and its wake without the inclusion of sizeable disturbances from the strut. However, useful overpressure disturbances from the nacelle's inlet lip and the curved forebody were readily obtained. In spite of these limitations on the boundary of the interference-free zone and the magnitude of the pressures in this interference-free zone, there were sufficient data for an evaluation of the flow-field overpressure prediction code at the near-field conditions available during the tests.

TEST SECTION AND APPARATUS

Flow-field overpressures generated by the nacelle model were measured in the wind-tunnel test section with the probes, models, and pressure gages arranged, approximately, as shown in figure 3.

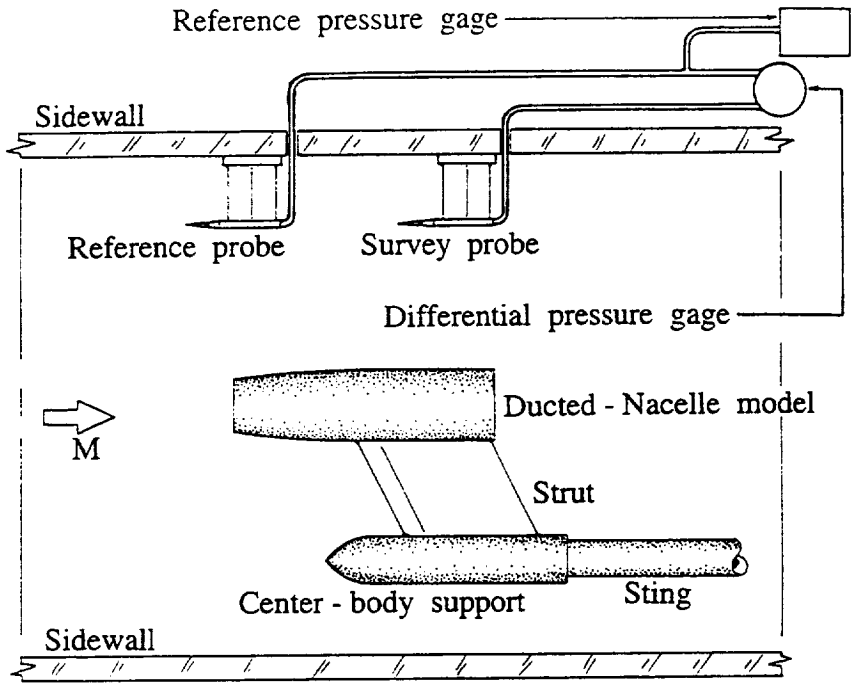

Figure 3. Schematic of wind-tunnel test section, model, and apparatus (not to scale).

Both the flow-field survey probe and the reference-pressure probe were cone-cylinder static pressure probes. The vertex angle was 4 degrees and the shaft diameter was 0.25 inches. Each probe had a pair of opposed 0.035 inch diameter orifices, located 1.25 inches aft of the cone vertex on the conical forebody, connected to a common channel passing through the cylindrical section. Differential pressures between the survey and the reference probes were measured with a 0.15 psid Statham differential-pressure gage mounted outside the test section. A separate gage measured reference-probe pressure to ratio with the differential pressure.

Gage limits were a factor that prevented the measurement of overpressures at extremely close distances. The gages were designed to function within a range of $-0.15 \leq \Delta p \leq 0.15$ psid although it was possible to modestly exceed these limits and still keep within the specified gage accuracy of ±0.5 percent of full scale. Since the static pressure changes with Mach number, the $\Delta p/p$ range limit for each Mach number varied also. These range limits are listed in Table II.

Table II. Pressure gage range limits, $\Delta p/p$ (max, min), at each of the test Mach numbers.

M	$\Delta p/p$ (max, min)
1.5	±0.075
1.8	±0.108
2.1	±0.151
2.4	±0.208

The quad-nacelle models' sting was fixed to the wind-tunnel's strut mechanism, and could be rotated so that shadowgraph pictures could be made of each nacelle. Spillage around the inlets of the nacelles as well as general flow quality over the exterior skin could be seen and photographed for analysis. During the subsequent flow-field overpressure measurements, the largest of the

nacelles, the 1:75 scale nacelle model, was set at different lateral distances to the survey probe in a plane normal to the wind-tunnel test section side wall. Overpressure signatures were measured by moving the model longitudinally forward or aft relative to the survey probe.

TEST CONDITIONS AND OBJECTIVES

The flow fields of the nacelle models were surveyed in Test Section 1 of the Langley Unitary Plan Wind Tunnel at supersonic-flow Mach numbers that varied with the area of study. Nacelle-inlet shock locations and possible inlet spillage were studied with shadowgraph pictures at Mach numbers of 2.3, 2.5, and 2.96, the Mach number range used in the wind-tunnel tests of two theory-validation wing-fuselage-nacelle models, reference 14. Test-section Reynolds number was 2 million per foot and the total temperature was maintained at 125 degrees Fahrenheit.

Flow-field overpressure signatures, generated by the 1:75 scale nacelle model, were measured at supersonic Mach numbers of 1.5, 1.8, 2.1, and 2.4. These Mach numbers spanned the range of interest for current civil supersonic-cruise aircraft concepts. Reynolds number per foot and total temperature conditions were the same as with the nacelle-inlet shock and spillage tests.

Inlet Spillage And Shock Tests. Shadowgraph pictures of the nacelles were made at Mach numbers of 2.3, 2.5, and 2.96. Angle of attack varied from 0.0 to 6.0 degrees at each of the test Mach numbers. This procedure was used to check the possibility that the wind-tunnel model nacelles suffered mass-flow choking in their under-the-wing position when pressure signatures from the wing-fuselage-nacelle models were measured. Shadowgraph pictures like the one in figure 4 were obtained and analyzed.

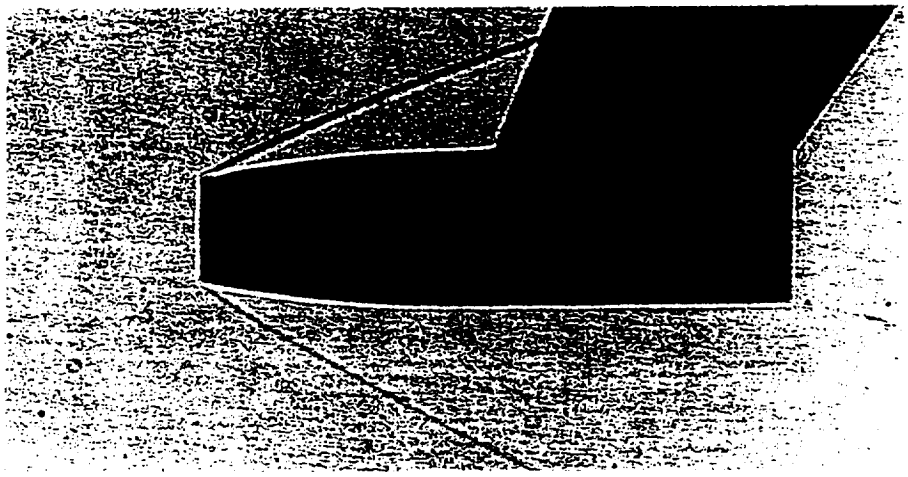

Figure 4. Sample shadowgraph picture of the 1:200 scale nacelle wind-tunnel model at M = 2.3 and zero angle of attack.

The shocks were attached to the nacelle inlet lip. This indicated that internal duct flow was not choked because little or no air spilled over the lip of the nacelle inlet. An almost-planar paraboloid shock was probably present across the lip diameter of the nacelle inlet, creating internal subsonic flow that accelerated, due to wall friction, through the nacelle's constant-area duct. There are also faint smudged lines from the back of the nacelle that indicated cylindrical

flow exiting the duct and merging with the air flowing over the nacelle's exterior surface. The lack of inlet spillage, and the signs of cylindrical exit flow, strongly reinforced the conclusion that the interior flow never reached sonic velocity within the duct. So, no choked flow occurred.

This pattern of attached inlet-lip shocks was also noticed on the other nacelle models, at the other test Mach numbers, and at all angles of attack used during the tests. It was concluded that spillage had not occurred with any of the nacelle models of this test, and none had occurred with the nacelles on the two theory-validation wing-fuselage models in a previous pressure-signature measurement test at similar Mach-Number/Reynolds-Number conditions.

Predictions from one-dimensional, constant-area, duct-flow theory, reference 15, were compared with the results from the wind-tunnel test pictures. At Mach 2.3, choked flow was predicted for a constant-area duct with a length/diameter ratio of about 30. Since the length/diameter ratio on the nacelle used in the test was 6.0, choking was not predicted. For Mach numbers of 2.5 and 2.96, the theory predicted choked flow when the length/diameter ratios were about 40 and 50, respectively. On the basis of this limited data sample, one-dimensional, constant-area, duct-flow theory appeared to be potentially useful for designing nacelles on sonic-boom wind-tunnel models that were about 12 inches or so in length.

Measured Pressure Signatures. Pressure signatures from the largest (1:75 scale) nacelle model were measured at Mach numbers of 1.5, 1.8, 2.1, and 2.4 with the Reynolds number per foot constant at 2 million. Separation distances varied from 2.27 inches to 13.27 inches. In most sonic-boom reports, the longitudinal distance along the pressure signature was normalized with the body length. Since the engine nacelles are often mounted very close to the lower wing surface, a different normalizing length was selected. For convenience, the inlet diameter was selected as this normalizing length since the distance between the nacelle and the interference region under the wing are usually convenient multiples of this dimension. With an inlet diameter of 0.96 inches, these (separation distance)/(diameter) ratios ranged from 2.36 to 13.82.

DATA REDUCTION

A sketch of a typical pressure signature generated by the 1:75 scale ducted-nacelle model and measured during the wind-tunnel tests is shown in figure 5.

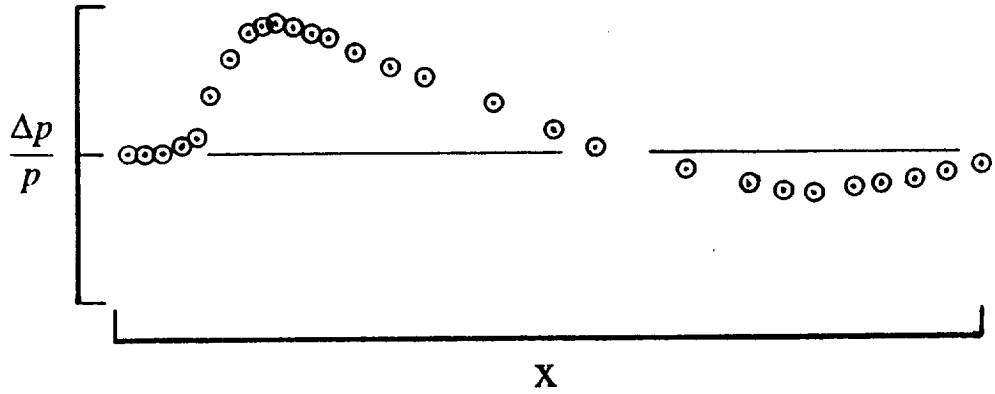

Figure 5. Typical measured pressure signature from the 1:75 scale ducted-nacelle model.

Wind-tunnel turbulence, model vibration, probe boundary layer, shallow shock angle, and finite orifice size on the survey probe spread the thin nose shock over a finite distance. An empirical technique, described in reference 16 and demonstrated in reference 13, was employed to adjust the wind-tunnel-measured nose shock in figure 5 to the idealized pressure-jump nose shock usually found in nature, figure 6.

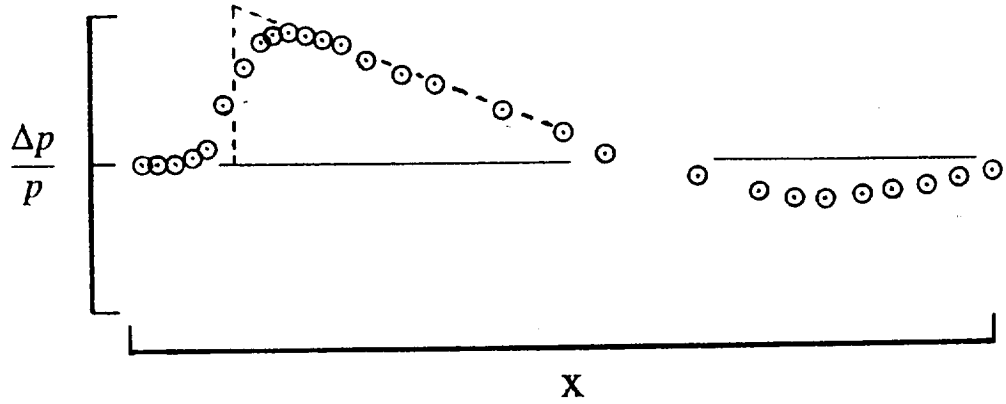

Figure 6. Pressure signature from figure 5, adjusted with the technique given in reference 16.

Two principles are followed in making this adjustment: (1) the total area under the positive-pressure section of the measured signature must be preserved; and (2) the "jump" from the ambient pressure to the peak pressure of the shock must take place over zero distance or zero time. When adjustments have been completed, the pressure signature in figure 6 can be compared with Whitham-theory predictions.

ANALYSIS OF EXPERIMENTAL DATA

Pressure signatures were predicted at each Mach number for a range of separation distances, and used for comparisons of nose-shock strength and pressure-signature shape. In reference 17, a correction, based on reference 18, to the usual low-disturbance sonic-boom predictions was introduced and discussed. The derivation of this correction is repeated from reference 17 in Appendix A. This correction has a Mach number factor and a pressure ratio factor to improve the accuracy of Whitham-theory pressure signature predictions. Two curves were obtained for comparison with experimental data: the first overpressure ratio prediction was calculated with the uncorrected first-order Whitham-theory equation, while the second prediction was derived from first-order Whitham theory with the correction factor included.

Nose-Shock Strength

As mentioned in the Pressure Signatures section, measurements were made at distances that ranged from 2.27 to 13.27 inches. Flow-field pressures over this full range were only obtained at Mach numbers of 1.5 and 1.8, but not at Mach numbers of 2.1 and 2.4 due to wind-tunnel apparatus limits. Maximum separation distance at Mach 2.1 was 6.27 inches; at Mach 2.4, it was 7.27 inches, both are greater than the nacelle length of 5.76 inches. A previous paper, reference 6, reported good agreement between theory and experiment at distances of 1 and 2 body lengths.

The minimum distance, $h / D_{min} = 0.50$, was set by the inlet radius of 0.48 inches. However, it was physically not possible to measure the inlet-lip shock strength at this close distance. The shock angles and shock strengths at each Mach number could be predicted from oblique-shock theory, reference 18, using the nacelle lip angle of 10.62 degrees. For comparison, predictions of shock strength at the inlet-lip were obtained from corrected and uncorrected Whitham theory. In figure 7, a comparison of results from these three calculations are shown.

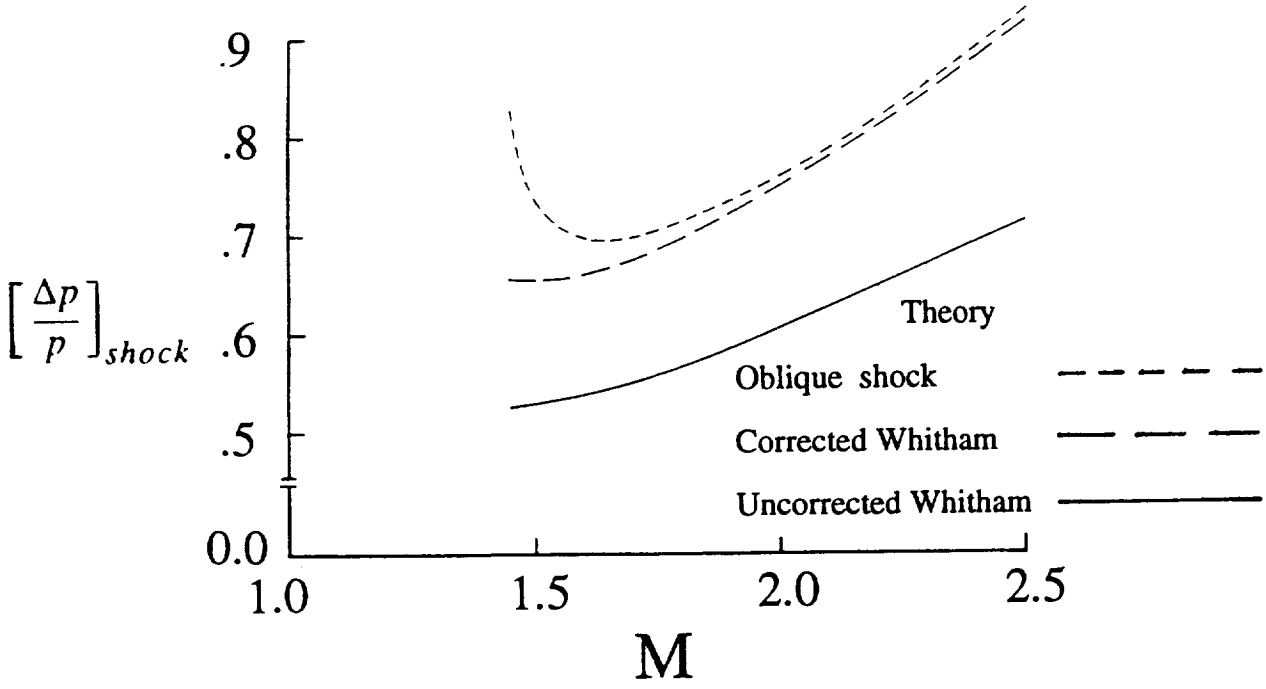

Figure 7. Comparison of nacelle-lip shock strengths predicted by oblique-shock and Whitham theories at Mach numbers from 1.45 to 2.5 for the nacelle lip angle, δ, of 10.62 deg.

For small deflection angles, oblique-shock theory predictions agreed well with experiment data. So, the relevance of this theory comparison was based on the evidence that shocks stayed attached to the nacelle lip even though the inlet lip angle on this nacelle model was larger than the 3.0 to 4.0 degrees usually found on full-sized engine nacelles. Good agreement between oblique-shock and corrected-Whitham theory in figure 7 was seen for Mach numbers greater than about 1.6. Since detached flow is predicted by oblique-shock theory below a Mach number of 1.45, no Whitham-theory solutions were presented.

Whitham-theory codes are used to compute nacelle-wing interference pressures in the zone bounded by the inlet-lip shock and the trailing edge. These interference pressures are used to compute lift, drag, and pitching moment increments. The data in figure 7 showed that Whitham-theory predictions would tend to underpredict near-field overpressures. With the empirical correction, the modified Whitham-theory predictions were in better agreement with oblique-shock theory (and by implication, in better agreement with real flow conditions). So this theory, in its modified form, has the potential of being useful in the estimation of nacelle-wing interference-lift force and moment increments on real aircraft.

In figures 8 to 11, two predicted nose-shock strength curves are compared with experimental data over the range of Mach numbers and separation distances. The nose-shock strengths were obtained from the experimental data with the methodology reported in reference 16, demonstrated

in reference 13, and shown in figure 6.

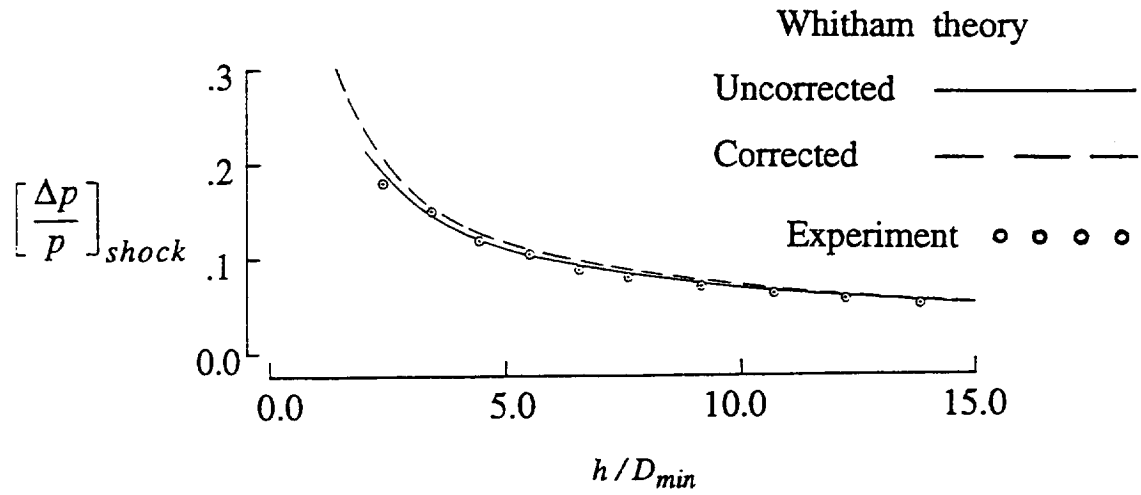

Figure 8. Comparison of measured and predicted nose-shock strengths at M = 1.50.

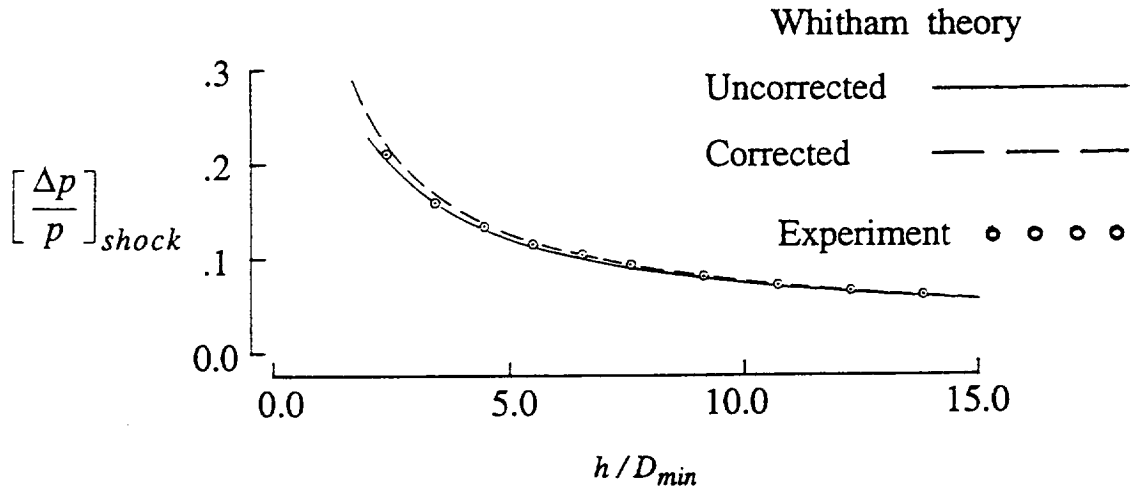

Figure 9. Comparison of measured and predicted nose-shock strengths at M = 1.80.

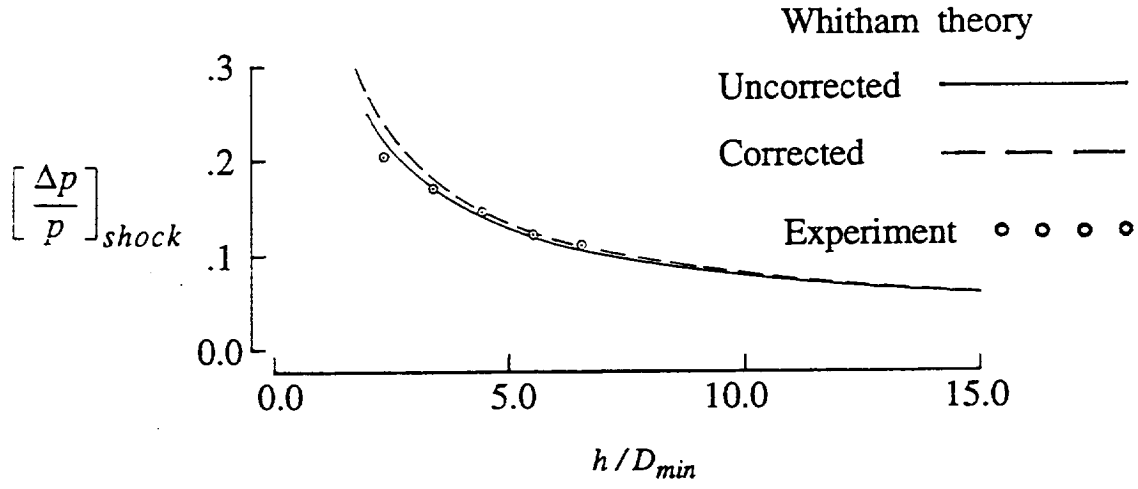

Figure 10. Comparison of measured and predicted nose-shock strengths at M = 2.10.

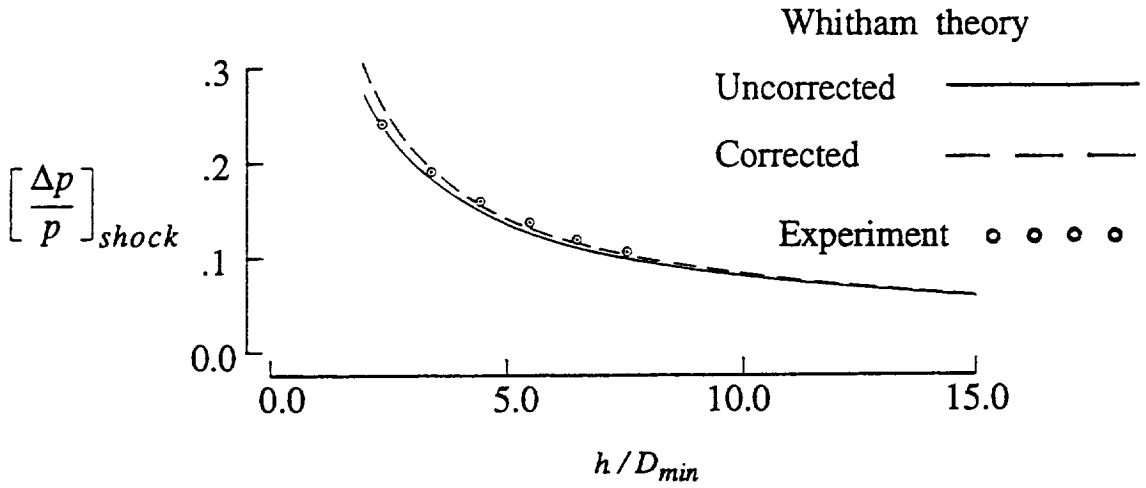

Figure 11. Comparison of measured and predicted nose-shock strengths at M = 2.40.

The agreement between the theoretical and experimental nose-shock strengths is generally good at $\Delta p/p$ values less than about 0.10. At higher values, the upwash from the oblique shock put increasing crossflow on the conical forebody of the probe, and degraded its capability to accurately measure static pressures. In figure 12, the theoretical flow angle behind an oblique shock is plotted versus Mach number and differential-pressure ratio $\Delta p/p$.

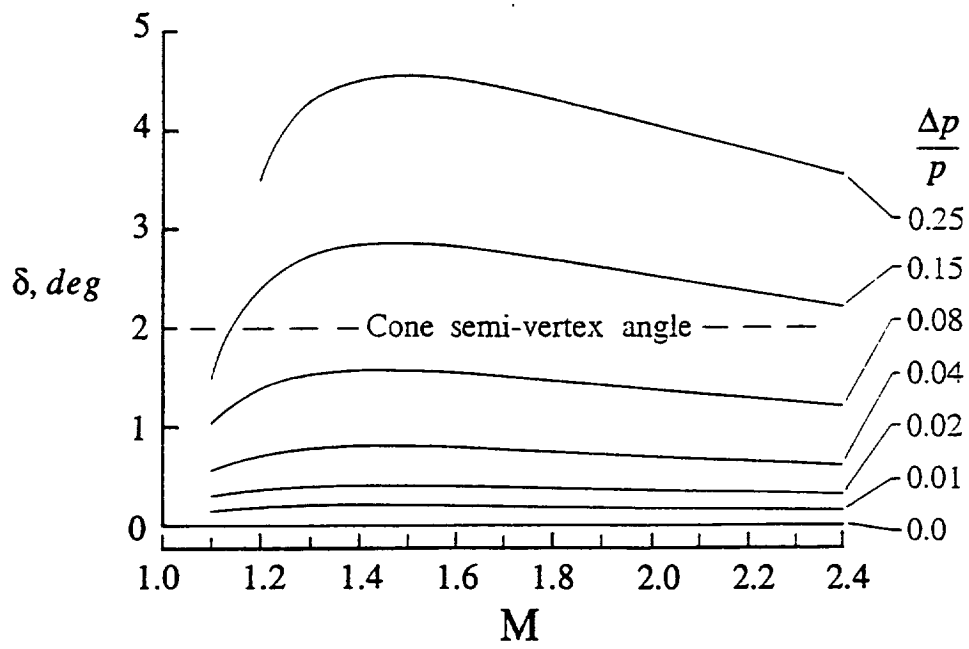

Figure 12. Predictions of shock-induced flow angle, δ, versus Mach number at various $\Delta p/p$.

Figure 3 in reference 13 shows the results of positioning a probe orifice at different attitudes in strong and weak overpressure fields. These data suggest that differences between theory and experiment at the higher pressure ratios can be attributed to both the theory and the measurement apparatus. While of little concern in sonic-boom wind-tunnel tests of concept models because the $\Delta p/p$ range nominally is: $-0.04 < \Delta p/p < 0.04$, it was of concern in these ducted-nacelle model

tests because all of the measured nose-shock $\Delta p/p$ were much larger than 0.040.

Pressure-Signature Shape

Agreement between measured and predicted nose-shock strength is important, but agreement between measured and predicted pressure-signature shape is also vital because it determines the accuracy of the interference-lift. Two flow-field regions will be considered separately: (1) extreme near-field - measurements made at the closest separation distance; and (2) mid-field - measurements made at the furthest separation distance. The wind-tunnel test section width precluded far-field measurements.

Near-field is often defined by separation distances of one or less body lengths. In this test, the closest separation distances were about 0.394 body lengths. Closer distances could not be reached due to the possibility of probe-model contact. Mid-field is a generic term applied to the region between the near field and the far field. The largest separation distance in the test was about 2.3 body lengths, obviously beyond near-field, but definitely not far-field.

For nacelles, however, the convenient length is minimum nacelle diameter because the engine inlets are usually located very close to the wing surface. So, in that frame of reference, the closest separation distances were about 2.365 diameters, and the largest separation distance was about 13.823 diameters which was representative of the distance from the nacelle to the wing tip. The near-field measurements are the most severe test of theory since the interference pressures are the highest, while the mid-field measurements will indicate how rapidly the interference pressures return to the low-disturbance conditions originally assumed in the framework of the theory. In the preceeding section, the near-field shock strengths were found to be strong enough to degrade the agreement between theory and experiment. It is expected that such trends will be carry over to comparisons of pressure signature shape.

Near-Field Comparisons. In figures 13 to 16, measured and predicted pressure signatures are compared for a range of Mach numbers at the closest nacelle-probe separation distance.

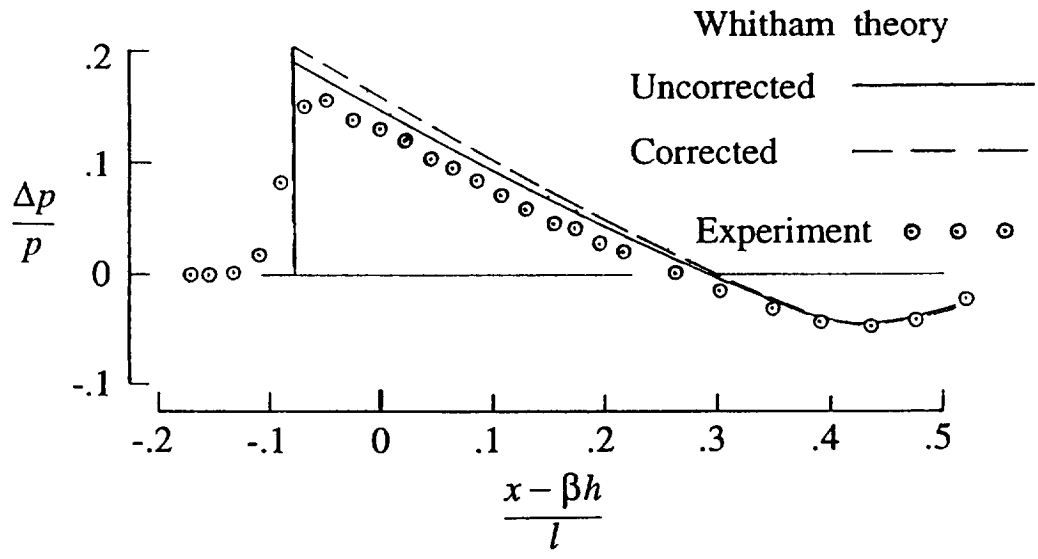

Figure 13. Comparison of measured and predicted near-field pressure signatures at M = 1.5, $h / D_{min} = 2.365$.

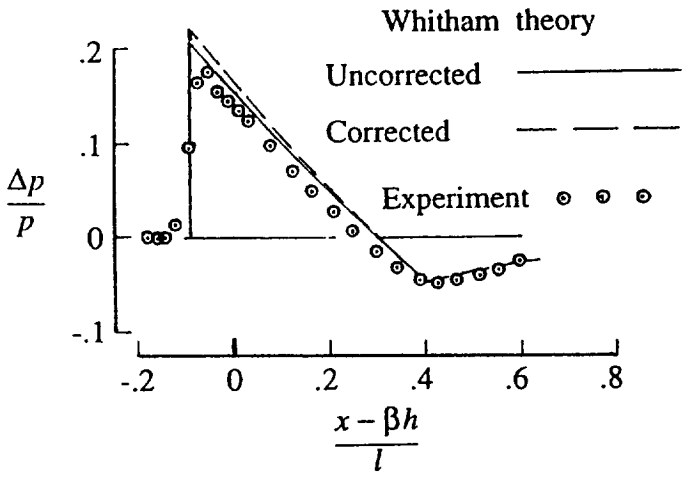

Figure 14. Comparison of measured and predicted near-field pressure signatures at M = 1.8, $h / D_{min} = 2.365$.

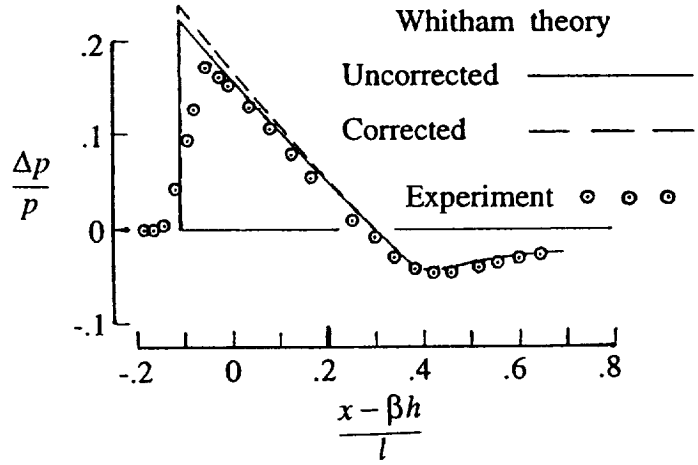

Figure 15. Comparison of measured and predicted near-field pressure signatures at M = 2.1, $h / D_{min} = 2.365$.

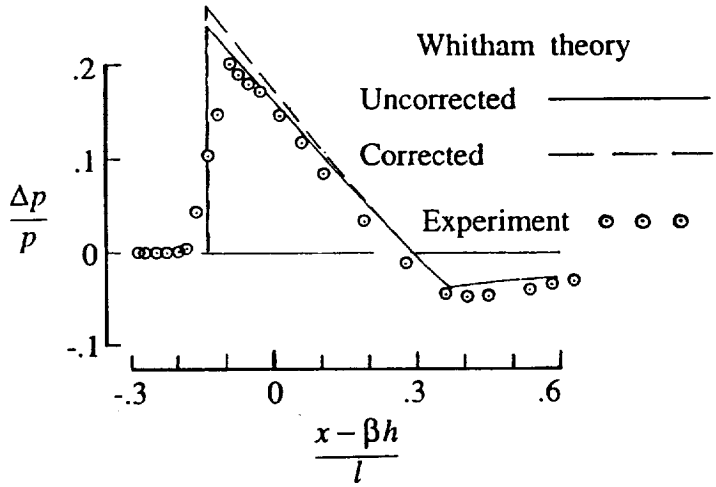

Figure 16. Comparison of measured and predicted near-field pressure signatures at M = 2.4, $h / D_{min} = 2.365$.

Mid-Field Comparisons. In figures 17 to 20, measured and predicted pressure signatures are compared for a range of Mach numbers at the furthest nacelle-probe separation distance.

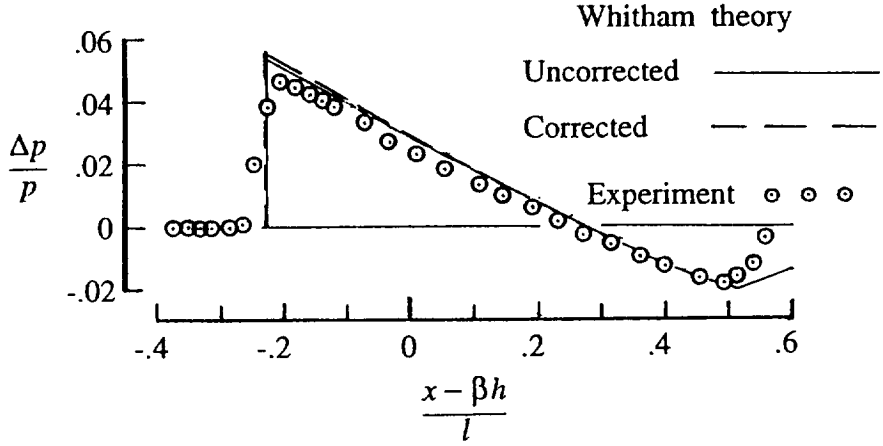

Figure 17. Comparison of measured and predicted mid-field pressure signatures at M = 1.5, $h / D_{min} = 13.823$.

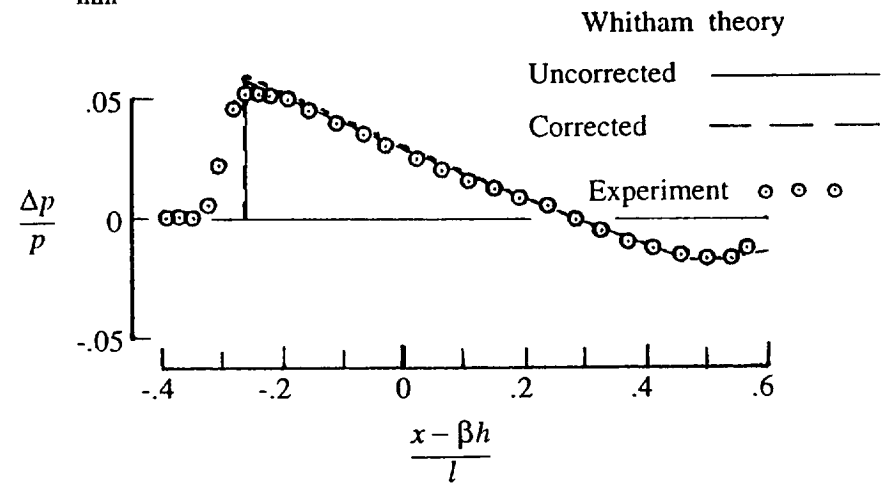

Figure 18. Comparison of measured and predicted mid-field pressure signatures at M = 1.8, $h / D_{min} = 13.823$.

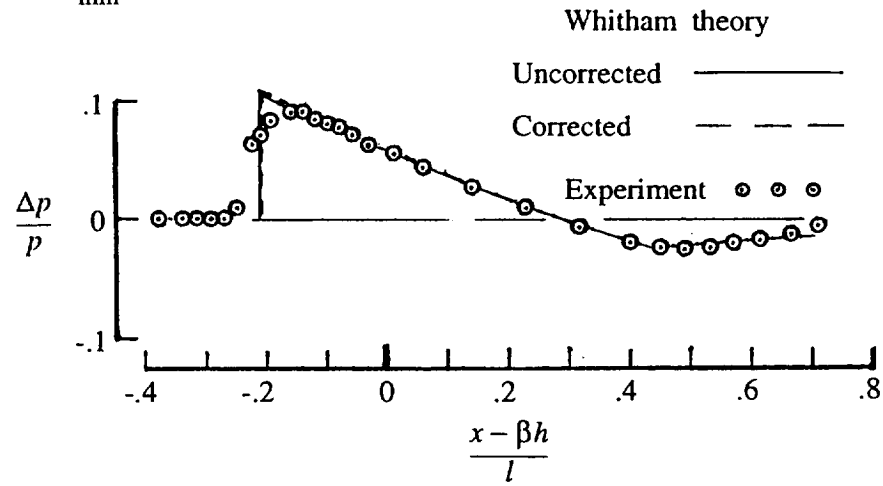

Figure 19. Comparison of measured and predicted mid-field pressure signatures at M = 2.1, $h / D_{min} = 6.531$.

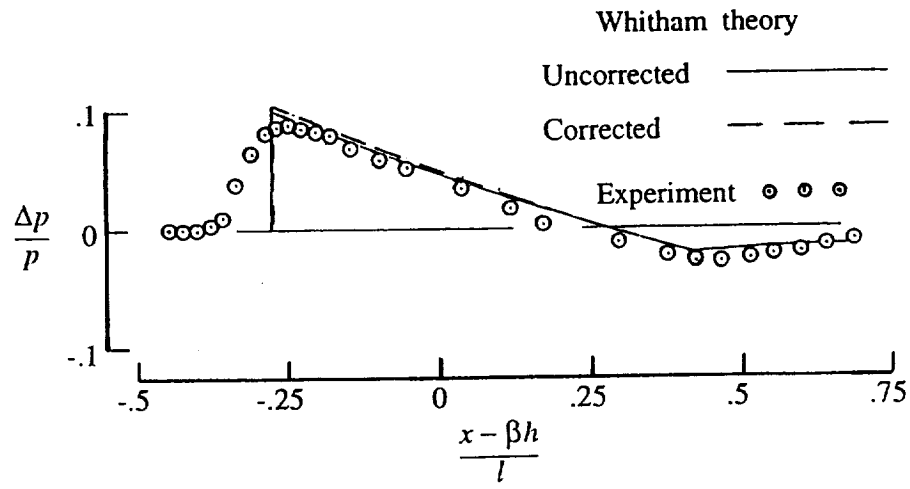

Figure 20. Comparison of measured and predicted mid-field pressure signatures at M = 2.4, $h / D_{min} = 7.573$.

Corrected and uncorrected Whitham theory slightly overpredicted the overpressures in the near-field, but predicted better in the mid-field. Data in Table II indicated that the measured overpressures were well above gage limits at Mach 1.5, but within gage limits at Mach 2.4.

DISCUSSION AND RESULTS

The shape of the pressure signatures in figures 13 to 20 might lead to the conclusion that the nacelle was generating far-field N-wave type disturbances. An analysis of the two Whitham F-functions shown in figure 21 shows that this is not the case.

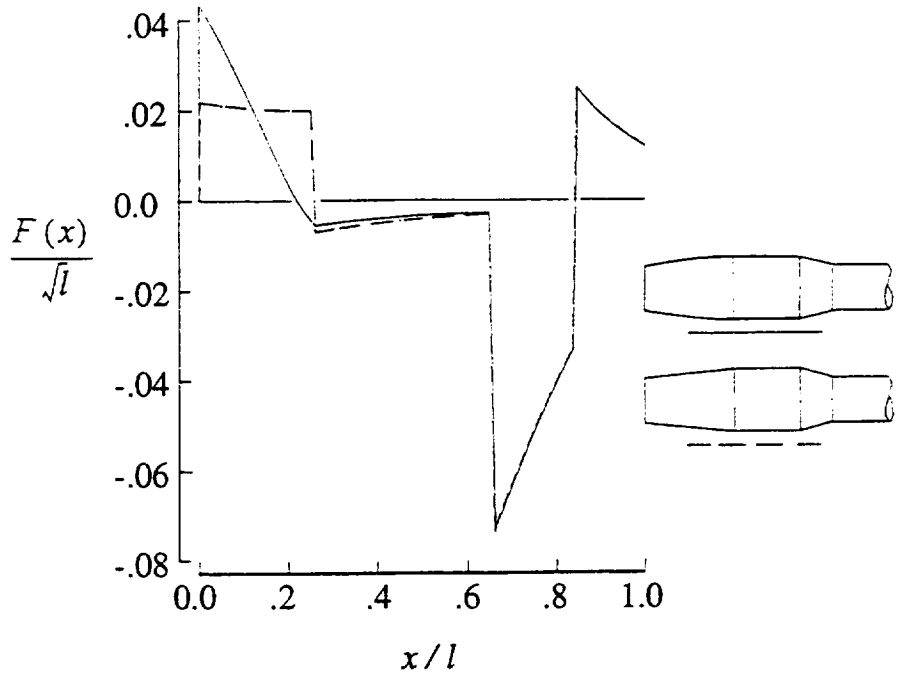

Figure 21. Comparison of Whitham F-functions from two similar nacelles at M = 2.4.

The F-function from the wind-tunnel nacelle model (shown in solid line) had an strong expansion which followed the initial shock at the lip. This F-function shape is typical for a tangent-ogive shape on a ducted-nacelle forebody. The second F-function is from a nacelle with the same inlet lip radius, same maximum body radius, and same forebody length, but with a truncated-cone forebody rather than a tangent-ogive forebody. Its magnitude decreased very little along the forebody length. After the expansion at the shoulder, the F-function decreased rapidly to nearly the same magnitude as that of the tangent-ogive forebody nacelle. The rest of both F-functions are virtually the same since both nacelles have the same arbitrary wakes following the nacelle exit. Thus, it is the forebody shape, not the fineness ratio on the wind-tunnel nacelle model, that gives the wind-tunnel test pressure signatures, figures 13 to 20, their decided far-field shape.

Exceeded gage limits might account for some of the less-than-good agreement between theory and experiment in the near-field at the test Mach numbers, figures 13 to 16, but flow angularity and its effect on gage accuracy should also be considered as contributory. If the trends in figure 7 were truly indicative of theory capabilities, corrected Whitham theory should *slightly underpredict*, rather than *overpredict* the magnitude of the overpressure. The fairly good agreement between theory and experiment at the test Mach numbers in the mid-field, figures 17 to 20, seems to support this conclusion. Therefore, the nacelle-wing interference lift code which employs this *corrected Whitham theory* should be capable of providing reasonably good estimates of incremental forces and pitching moment during the preliminary design phase of conceptual aircraft development, and useful interference-lift equivalent areas for the sonic-boom analysis.

CONCLUDING REMARKS

An experimental and theoretical study of the flow field around ducted-nacelle wind-tunnel models has been presented. Shadowgraph pictures of four different-scale ducted-nacelle models showed attached inlet-lip shocks and no signs of choked flow over an angle of attack range of 0 to 6 degrees for Mach numbers of 2.3, 2.5, and 2.96. Thus, it was concluded that the flow through the constant-area ducts of these *1:75 to 1:200 scale* nacelles was unchoked. The one-dimensional constant-area duct theory used to predict flow quality in the constant-area duct of the nacelle agreed with these results since it also predicted unchoked flow.

However, the nacelles used on *1:300 scale* wind-tunnel models of HSCT concepts were 50 percent smaller and would be positioned under a model wing rather than in unobstructed air flow. The limited-sample validation of constant-area duct theory by the results of the wind-tunnel measurements suggested that this theory could be useful in the prediction of flow quality through the smaller nacelles on the model when the flow-field velocities under the wing are determined at least to first order by supersonic-speed wing-performance codes.

Comparisons of measured and predicted flow-field overpressures around the forebody of the largest of the four ducted-nacelle models were also presented and analyzed. Test Mach numbers of 1.5, 1.8, 2.1, and 2.4, and separation distances that ranged from 2.365 to 13.823 inlet diameters represented the flow-field distances found between the nacelles and the edges of the interference-lift zone under many supersonic-cruise concepts currently under study. Reasonable agreement between theory and experiment was found with the near-field overpressure signatures if allowances were made for the effects of shock-induced flow angularity and the measurement of differential pressures that, at times, exceeded pressure-gage limits. Good agreement between theory and experiment was found with overpressure signatures measured at the largest separation

distances, where Whitham theory and corrected Whitham theory is most appropriate. The results supported the conclusion that corrected Whitham theory could predict incremental nacelle-wing interference lift forces and pitching moment reasonably well to merit its use both in preliminary conceptual aircraft design and analysis, as well as in sonic-boom analysis of aircraft flying at supersonic speeds.

REFERENCES

1. Harris, Roy V., Jr.: *A Numerical Technique For Analysis Of Wave Drag At Lifting Conditions*. NASA TN D-3586, 1966.

2. Carlson, Harry W.; and Miller, David S.: *Numerical Methods For The Design and Analysis Of Wings At Supersonic Speeds*. NASA TN D-7713, 1974.

3. Sommer, Simon C.; and Short, Barbara J.: *Free-Flight Measurements Of Turbulent-Boundary-Layer Skin Friction In The Presence Of Severe Aerodynamic Heating At Mach Numbers From 2.8 to 7.0*. NACA TN 3391, 1955.

4. Sorrells, Russell B.; and Miller, David S.: *Numerical Method For Design Of Minimum-Drag Supersonic Wing Camber With Constraints On Pitching Moment And Surface Deformation*. NASA TN D-7097, 1972.

5. Carlson, Harry W.; and Mack, Robert J.: *Estimation Of Wing Nonlinear Aerodynamic Characteristics At Supersonic Speeds*. NASA TP 1718, 1980.

6. Mack, Robert J.: *A Numerical Method For Evaluation And Utilization Of Supersonic Nacelle-Wing Interference*. NASA TN D-5057, 1969.

7. Middleton, W. D.; and Lundry, J. L.: *Aerodynamic Design And Analysis System For Supersonic Aircraft*. Boeing Commercial Airplane Company, NASA CR-2520, 1975.

8. Whitham, G. B.: *The Flow Pattern Of A Supersonic Projectile*. Communication on Pure and Applied Mathematics, vol.V, no. 3, Aug. 1952, pp. 301-348.

9. Middleton, Wilbur D.; and Carlson, Harry W.: *A Numerical Method For Calculating Near-Field Sonic-Boom Pressure Signatures*. NASA TN D-3082, 1965.

10. Carlson, Harry W.; Mack, Robert J.; and Morris, Odell A.: *A Wind-Tunnel Investigation Of The Effect Of Body Shape On Sonic-Boom Pressure Distributions*. NASA TN D-3106, 1965.

11. Shrout, Barrett L.; Mack, Robert J,; and Dollyhigh, Samuel M.: *A Wind-Tunnel Investigation Of Sonic-Boom Pressure Distributions Of Bodies Of Revolution At Mach 2.96, 3.83, and 4.63*. NASA TN D-6195, 1971.

12. Mack, Robert J.: *A Study Of Methods Which Predict Supersonic Flow Fields From Body*

Geometry, Distance, And Mach Number. NASA TN D-7387, 1973.

13. Carlson, Harry W.; and Mack, Robert J.: *A Study Of The Sonic-Boom Characteristics Of A Blunt Body At A Mach Number Of 4.14.* NASA TP 1015, 1977.

14. Mack, R.; and Needleman, K.: *The Design Of Two Sonic-Boom Wind-Tunnel Models From Conceptual Aircraft Which Cruise At Mach Numbers Of 2.0 And 3.0.* Thirteenth AIAA Conference, Tallahassee Florida, October 22-24, 1990.

15. Cambel, Ali B.; and Jennings, Burgess H.: Gas Dynamics, McGraw-Hill Book Company Inc., New York, 1958.

16. Carlson, Harry W.: *Correlation Of Sonic-Boom Theory With Wind-Tunnel And Flight Measurements.* NASA TR R-213, 1964.

17. Mack, Robert J.: *Some Considerations On The Integration Of Engine Nacelles Into Low-Boom Aircraft Concepts.* High-Speed Research: Sonic Boom, Volume II, NASA Conference Publications 3173, 1992.

18. Ames Research Staff; *Equations, Tables, And Charts For Compressible Flow.* NACA Report 1135, 1953.

APPENDIX A

WHITHAM-THEORY AND MACH-NUMBER CORRECTIONS TO THE PREDICTION OF OVERPRESSURE RATIO

Whitham theory, reference 8, used simple perturbation theory to predict the overpressure-to-ambient pressure ratio as

$$\frac{\Delta p}{p} = \frac{\gamma M^2}{\sqrt{2\beta r}} \Delta F(y) \tag{A1}$$

If ξ is defined as the quantity

$$\xi = \frac{\gamma M^2 \delta}{\beta} \tag{A2}$$

and is used in equations (151) and (174) of reference 18, then the overpressure ratio can be written as - omitting the term in ξ^3

$$\frac{\Delta p}{p} = \xi + \kappa \xi^2 \tag{A3}$$

where

$$\kappa = \frac{(\gamma + 1.0) M^4 - 4\beta^2}{4\gamma \beta^2 M^2} \tag{A4}$$

The variable ξ is an linear-theory estimate of incremental overpressure based on flow deflection. If it is replaced, in equation (A3), by its Whitham-theory counterpart in equation (1)

$$\xi = \frac{\gamma M^2}{\sqrt{2\beta r}} \Delta F(y) \tag{A5}$$

then, a corrected Whitham-theory prediction for the overpressure ratio can be written with equations A3), (A4), and (A5) as:

$$\frac{\Delta p}{p} \approx \xi + \kappa \xi^2 \tag{A6}$$

In equations (A2) and (A3), the variable δ is the change in flow angle through a shock, but it can also be used, in the more general sense, as the incremental angle, in the flow field, induced by the presence of the perturbing body. Whitham theory can be employed to predict this flow-angle increment in terms of the F-function, F(y). So the use of equations (A2) to (A5) enables equation (A6) to have corrections based on both first-order estimates of the overpressure from Whitham theory, and corrections based on the Mach number. Since it is used for both compressions and expansions, equation (A6) should be accurate to second order. The text shows comparisons of measured overpressure ratio with the overpressure ratios predicted by equations (A1) and (A6).

REPORT DOCUMENTATION PAGE

Form Approved
OMB No. 0704-0188

1. AGENCY USE ONLY (Leave blank)	2. REPORT DATE	3. REPORT TYPE AND DATES COVERED
	May 1998	Technical Memorandum

4. TITLE AND SUBTITLE
Experimental and Theoretical Study of Flow Fields Around Ducted-Nacelle Models

5. FUNDING NUMBERS
WU 537-07-21-21

6. AUTHOR(S)
Robert J. Mack

7. PERFORMING ORGANIZATION NAME(S) AND ADDRESS(ES)
NASA Langley Research Center
Hampton, VA 23681-2199

8. PERFORMING ORGANIZATION REPORT NUMBER
L-17741

9. SPONSORING/MONITORING AGENCY NAME(S) AND ADDRESS(ES)
National Aeronautics and Space Administration
Washington, DC 20546-0001

10. SPONSORING/MONITORING AGENCY REPORT NUMBER
NASA/TM-1998-207683

11. SUPPLEMENTARY NOTES

12a. DISTRIBUTION/AVAILABILITY STATEMENT
Unclassified-Unlimited
Subject Category 05 Distribution: Nonstandard
Availability: NASA CASI (301) 621-0390

12b. DISTRIBUTION CODE

13. ABSTRACT *(Maximum 200 words)*

The flow field near four small-scale ducted-nacelle bodies of revolution has been analytically and experimentally studied to determine exterior and interior mass-flow characteristics, and to measure flow-field overpressures generated by the nacelle's forebody shape. Four nacelle models with the same profile, but of different sizes, were used in the study. Shadowgraph pictures showed inlet shocks attached to the cowl lip (indicating unchoked flow) on all four models, at all the test Mach numbers, through an angle of attack range of 0.0 to 6.0 degrees. Pressure signatures measured in the flow field of the largest of the four nacelle models were compared with those predicted by corrected and uncorrected Whitham theory. At separation distances greater than 3.0 to 4.0 inlet diameters, good agreement was found. Poorer agreement was found at extreme near-field separation distances, but this was attributed to pressure-gage limitations and probe-flow field interactions. The overall favorable results supported a conclusion that corrected Whitham theory was sufficiently accurate to make the nacelle-wing interference-lift code useful for sonic-boom analysis and the preliminary design of supersonic-cruise conceptual aircraft.

14. SUBJECT TERMS
Ducted nacelles; Supersonic flow; Flow-field overpressures; Wind-tunnel test; Whitham-theory analysis

15. NUMBER OF PAGES
25

16. PRICE CODE
A03

17. SECURITY CLASSIFICATION OF REPORT	18. SECURITY CLASSIFICATION OF THIS PAGE	19. SECURITY CLASSIFICATION OF ABSTRACT	20. LIMITATION OF ABSTRACT
Unclassified	Unclassified	Unclassified	